



**HAL**  
open science

## **BeStSel: a web server for accurate protein secondary structure prediction and fold recognition from the circular dichroism spectra**

András Micsonai, Frank Wien, Éva Bulyáki, Judit Kun, Éva Moussong, Young-Ho Lee, Yuji Goto, Matthieu Réfrégiers, József Kardos

### ► To cite this version:

András Micsonai, Frank Wien, Éva Bulyáki, Judit Kun, Éva Moussong, et al.. BeStSel: a web server for accurate protein secondary structure prediction and fold recognition from the circular dichroism spectra. *Nucleic Acids Research*, 2018. hal-01824353

**HAL Id: hal-01824353**

**<https://hal.science/hal-01824353>**

Submitted on 27 Jun 2018

**HAL** is a multi-disciplinary open access archive for the deposit and dissemination of scientific research documents, whether they are published or not. The documents may come from teaching and research institutions in France or abroad, or from public or private research centers.

L'archive ouverte pluridisciplinaire **HAL**, est destinée au dépôt et à la diffusion de documents scientifiques de niveau recherche, publiés ou non, émanant des établissements d'enseignement et de recherche français ou étrangers, des laboratoires publics ou privés.

# BeStSel: a web server for accurate protein secondary structure prediction and fold recognition from the circular dichroism spectra

András Micsonai<sup>1</sup>, Frank Wien<sup>2</sup>, Éva Bulyáki<sup>1</sup>, Judit Kun<sup>1</sup>, Éva Moussong<sup>1</sup>, Young-Ho Lee<sup>3</sup>, Yuji Goto<sup>3</sup>, Matthieu Réfrégiers<sup>2</sup> and József Kardos<sup>1,\*</sup>

<sup>1</sup>ELTE NAP Neuroimmunology Research Group, Department of Biochemistry, ELTE Eötvös Loránd University, Budapest H-1117, Hungary, <sup>2</sup>Synchrotron SOLEIL, Gif-sur-Yvette 91192, France and <sup>3</sup>Institute for Protein Research, Osaka University, Osaka 565-0871, Japan

Received February 24, 2018; Revised May 17, 2018; Editorial Decision May 18, 2018; Accepted May 22, 2018

## ABSTRACT

Circular dichroism (CD) spectroscopy is a widely used method to study the protein secondary structure. However, for decades, the general opinion was that the correct estimation of  $\beta$ -sheet content is challenging because of the large spectral and structural diversity of  $\beta$ -sheets. Recently, we showed that the orientation and twisting of  $\beta$ -sheets account for the observed spectral diversity, and developed a new method to estimate accurately the secondary structure (PNAS, 112, E3095). BeStSel web server provides the Beta Structure Selection method to analyze the CD spectra recorded by conventional or synchrotron radiation CD equipment. Both normalized and measured data can be uploaded to the server either as a single spectrum or series of spectra. The originality of BeStSel is that it carries out a detailed secondary structure analysis providing information on eight secondary structure components including parallel- $\beta$  structure and antiparallel  $\beta$ -sheets with three different groups of twist. Based on these, it predicts the protein fold down to the topology/homology level of the CATH protein fold classification. The server also provides a module to analyze the structures deposited in the PDB for BeStSel secondary structure contents in relation to Dictionary of Secondary Structure of Proteins data. The BeStSel server is freely accessible at <http://bestsel.elte.hu>.

## INTRODUCTION

Circular dichroism (CD) spectroscopy is a widely used spectroscopic technique that measures the differential absorption between left and right circularly polarized light. In pro-

teins, the peptide bonds contribute mostly to the far-UV CD spectrum between 170 and 250 nm. It was observed already 50 years ago that different proteins can exhibit distinct spectral profiles (1) depending on the conformation and environment of the peptide bonds and their H-bonding pattern, which are characteristic to the secondary structure of the proteins. With the development of the instrumentation, conventional benchtop CD instruments have become widely available. Moreover, the setup of synchrotron radiation CD spectroscopy provides a broad wavelength range and low noise for high quality CD spectra (2). In structural biology, the number of atomic resolution protein structures has been increased rapidly and more and more of them had their CD spectra recorded. These reference spectra of proteins with known structures stimulated the construction of a variety of algorithms to analyze the CD spectra to gain secondary structure information. These methods distinguish three–six secondary structure components, which are most often helix,  $\beta$ -sheet, turn and ‘others’ (disordered) (3–9). They predict the helix content more-or-less accurately, while often fail to predict the  $\beta$ -sheet content.  $\beta$ -sheets can largely differ in the parallel-antiparallel orientation, in the length and number of strands and in their twists. This structural variety is manifested in the CD spectral diversity which has been generally believed to be an inherent limitation for the secondary structure estimation (10). The worst examples were the amyloid fibrils having high  $\beta$ -sheet content which was predicted as helix by most of the previously available methods (11). The spectral diversity of proteins having similar amount of different type of  $\beta$ -structures is presented in Figure 1. Investigating this problem we have shown recently that the parallel-antiparallel orientation and the twist of the  $\beta$ -sheets account for the observed spectral diversity of  $\beta$ -sheets (11). We have developed a new method, BeStSel (Beta Structure Selection), that takes into account the orientation and twist of the  $\beta$ -sheets and provides improved accuracy on a broader range of protein structures includ-

\*To whom correspondence should be addressed. J. Kardos. Tel: +36 1 372 2500/1795; Fax: +36 1 381 2172; E-mail: kardos@elte.hu

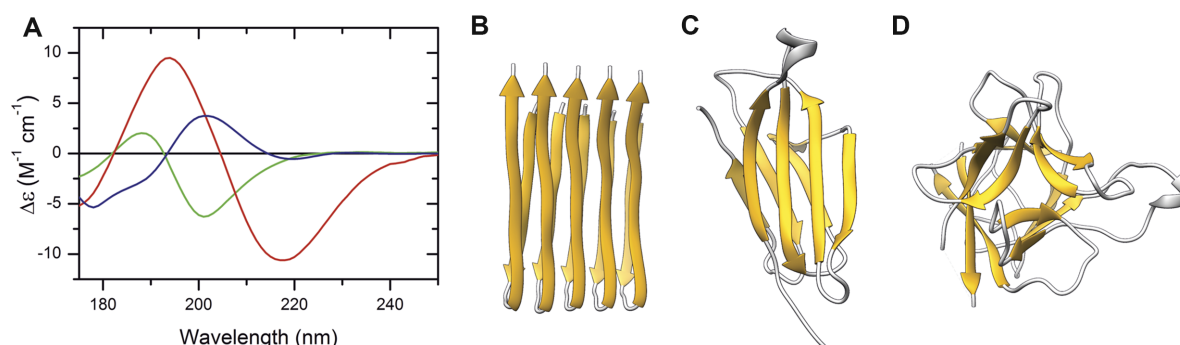


**Figure 1.** Spectral and structural diversity of mainly  $\beta$ -structured proteins. (A) CD spectra of  $\beta$ -amyloid (1–42) fibrils (red), native  $\beta_2$ -microglobulin (b2m, blue) and soybean trypsin inhibitor (SBTI, green) downloaded from PCDDDB (40). (B) Solid-state NMR model (PDB ID: 2BEG, (41)) of amyloid- $\beta$  fibrils consisting of parallel  $\beta$ -sheets, (C) relaxed (slightly right-hand twisted) antiparallel  $\beta$ -sheets of b2m (PDB ID: 2YXF, (42)) and (D) highly right-hand twisted antiparallel  $\beta$ -structure of SBTI (PDB ID: 1BA7, (43)). Previously available methods had difficulties with quantitative analyses of these spectra and their structural distinction, especially that of the amyloid fibrils (11).

ing  $\beta$ -sheet-rich proteins, membrane proteins, protein aggregates and amyloid fibrils. The method estimates even  $\alpha$ -helix content more accurately than previous methods but its strength is that it provides detailed information on the  $\beta$ -sheets, distinguishing parallel  $\beta$ -sheets and antiparallel  $\beta$ -sheets with three different twists, left-hand twisted, relaxed (slightly right-hand twisted) and right-hand twisted (11). The secondary structure components of BeStSel are presented in Figure 2. We have also shown for the first time, that this increased structural information gained from the CD spectrum makes possible the prediction of the protein fold down to the topology level using the CATH fold classification (12). A web server was constructed at <http://bestsel.elte.hu> making the BeStSel method freely accessible for the scientific community. It is indispensable when a quick and reliable structure analysis is needed and especially useful when X-ray crystallography or nuclear magnetic resonance (NMR) are not feasible.

## MATERIALS AND METHODS (WEB SERVER DESCRIPTION)

### Secondary structure elements of BeStSel and the twist of $\beta$ -sheets

Eight secondary structure elements are defined in BeStSel based on Dictionary of Secondary Structure of Proteins (DSSP (13)) as presented in Figure 2. Residues assigned to  $\alpha$ -helix by DSSP are divided into two groups, regular, and distorted, as the middle part of  $\alpha$ -helices (Helix1) and two residues at both ends of  $\alpha$ -helices (Helix2), respectively. The overall  $\beta$ -sheet content was determined by the fraction of the residues assigned to  $\beta$ -strand by DSSP. Parallel  $\beta$ -sheets are distinguished from antiparallel ones. The twisting angles for  $\beta$ -sheets are determined as the angles between the peptide backbones of two neighboring  $\beta$ -strands at the locations of pairs of adjacent residues along the neighboring  $\beta$ -strands as adapted from Ho and Curmi (11,14). According to the twisting angles, the antiparallel  $\beta$ -sheet content was divided into three groups using  $+3^\circ$  and  $+23^\circ$  as boundaries between the groups named left-hand twisted (Anti1), relaxed (slightly right-hand twisted, Anti2) and right-hand twisted (Anti3). Turn in BeStSel is defined identically to that

in DSSP (13). All other residues, including invisible ones in the three-dimensional structures, are assigned to ‘Others’.

### CD spectrum reference sets and basis spectra of BeStSel

A reference CD spectrum set of 73 proteins with known 3D-structures was used to optimize the BeStSel basis spectra. The reference set consisted of the spectra of the SP175 SRCD reference set of PCDDDB (15) and some additional  $\beta$ -structure-rich spectra that were also deposited in PCDDDB (see Micsonai *et al.* (11)). Another set of proteins was used as an independent test set of  $\beta$ -structure-rich proteins or proteins with rare secondary structure composition (11).

For the secondary structure determination, BeStSel uses the pre-calculated, fixed basis spectrum sets by fitting the CD spectrum of any unknown protein with the linear combination of the basis spectra (11). Each set contains eight basis spectra for the eight secondary structure components. However, each basis spectrum set is optimized separately for one of the secondary structure components, e.g. Helix1 content is determined using the basis spectra optimized to provide the best results on Helix1, and taken as the Helix1 fraction from the fitting. The other seven secondary structure contents are determined similarly from the other seven fittings. In each case, the basis spectra were calculated by least squares method on an optimized reference spectrum and wavelength data subset. The entire optimization process was separately executed for the different wavelength ranges offered by the BeStSel server (175–250, 180–250, 190–250 and 200–250 nm). The optimization procedure to get the basis spectra sets is described in details by Micsonai *et al.* (11).

### Protein fold prediction by BeStSel

The criteria for a successful fold recognition from the secondary structure contents is that the secondary structure elements and their composition should be characteristic to the protein fold. Two proteins with similar secondary structure composition and chain length should have similar folds. A simple secondary structure decomposition with three components, such as helix,  $\beta$ -sheet and ‘others’ is obviously insufficient for protein fold characterization, mainly

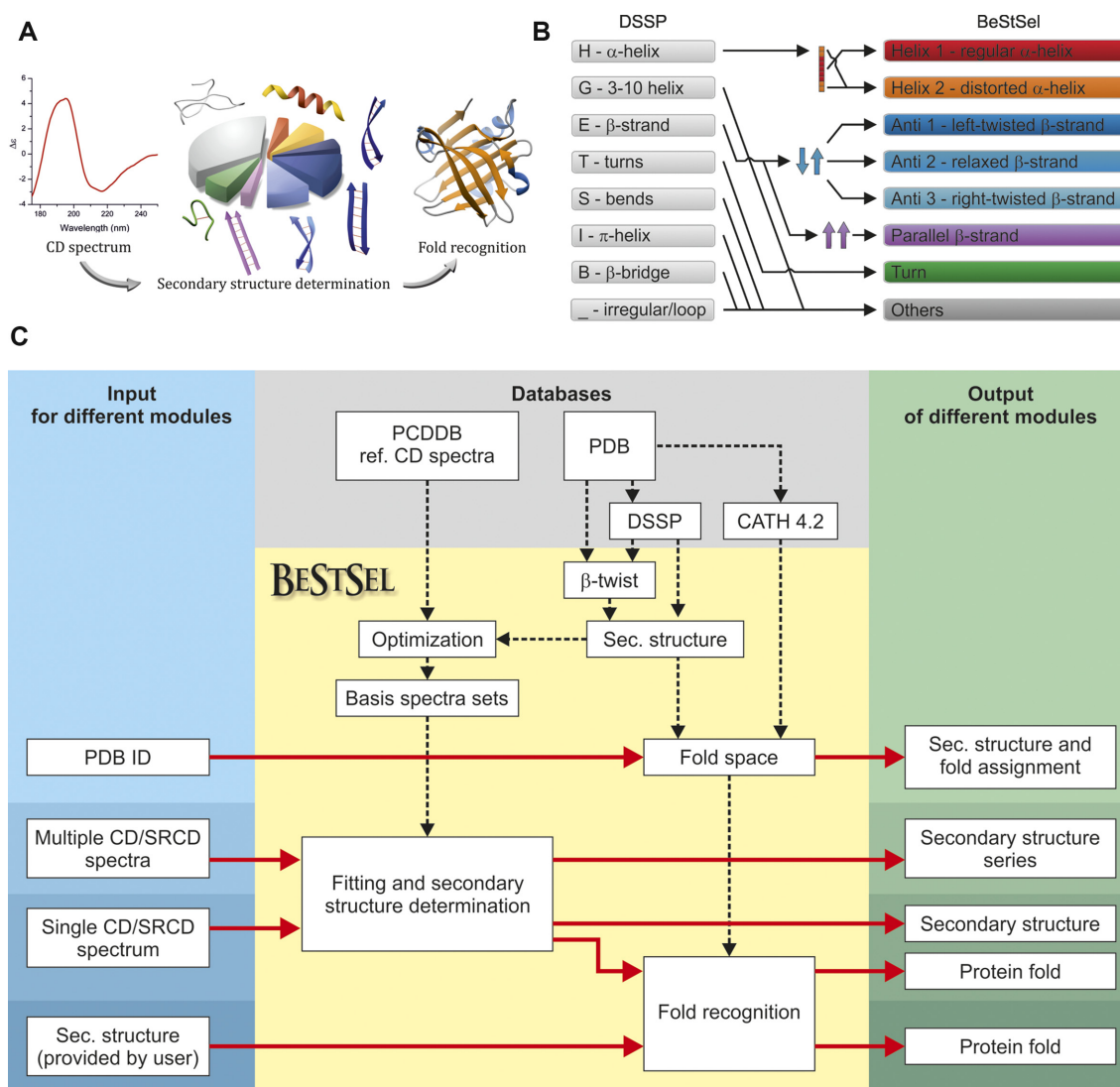


**Figure 2.** The framework of the BeStSel server. (A) Schematic representation of CD spectrum analysis. First, the secondary structure contents are determined for the eight components of BeStSel. Then, based on the secondary structure composition a search can be carried out for the most similar structures in the dataset derived from PDB and find out their fold classification. (B) Secondary structure elements defined in BeStSel as derived from DSSP. The regular, middle part of an  $\alpha$ -helix is distinguished from the ends (distorted helix),  $\beta$ -sheets are divided into four groups, parallel  $\beta$ -sheets and antiparallel left-hand twisted, regular and right-hand twisted  $\beta$ -sheets. Turn component covers the  $\beta$ -turns, and the 'Others' represent the rest of the structural elements and the irregular or disordered structures. (C) Block diagram showing the modules and functions of the BeStSel package. Input data are on the left, output data presented on the right. From a single CD spectrum the secondary structure contents are estimated and then, based on these, the protein fold can be predicted. A series of CD spectra as input can be evaluated at once to get the secondary structure contents. Users can provide arbitrary secondary structure contents and carry out the fold prediction for that secondary structure composition. Users can also enter PDB IDs as input to find out the corresponding secondary structure contents and fold classification.

because of the diversity of  $\beta$ -structures, which vary from parallel  $\beta$ -sheets and  $\beta$ -helices to antiparallel plain  $\beta$ -sheets,  $\beta$ -barrels, highly twisted structures and their combinations.  $\alpha$ -helical folds can be specified by the number and length of helices, which cannot be revealed by a single overall  $\alpha$ -helix content. The eight secondary structure elements of BeStSel are better descriptors of the protein structure and suitable for fold prediction (11). Intriguingly, DSSP, which also provides eight secondary structure components, is less characteristic to the protein fold containing several components which are less related to the protein fold, such as the bends,  $\beta$ -bridges and  $\pi$ -helices. In the BeStSel package,

the CATH protein fold classification is used (12), which distinguishes several hierarchical levels of protein fold, starting from the class to architecture, topology, homology (superfamily) and further levels. Every single protein structure can be represented by a point in the eight-dimensional secondary structure space of BeStSel. The distance between two points is defined by their Euclidean distance. The search for the protein fold corresponding to a secondary structure composition is based on the CATH classifications of the protein structures deposited in the PDB, i.e. we search for structures in the PDB that have similar secondary structure composition to the result of the CD analysis and then



discover their folds. Even in the case of using the BeStSel secondary structure components, protein folds can be overlapping in the eight-dimensional secondary structure space making the fold prediction challenging. Depending on the secondary structure composition (see below), different prediction methods can be effective. If the protein of interest is a multidomain protein containing heterodomains, there is much less chance for a clear prediction. The BeStSel package offers various different methods for fold recognition. The simplest method makes a search on the entire PDB and sorts out the twenty closest structures regarding the Euclidean distance from the secondary structure of interest in the eight-dimensional space. The CATH classification of the resulting structures are listed out and the user can examine these structures by using additional external information, e.g. chain length and sequence information. In the case of single domain proteins, we use a reference database that contains the non-redundant (95% sequence identity is allowed) single domain reference subset of CATH 4.2 (16) and the corresponding secondary structure compositions calculated from the respecting PDB structures. This database contains 55350 chains (domains) covering the four fold classes, 41 architectures, 1310 topologies and 5398 homologies. Three different methods are available for prediction of single domain proteins: (i) BeStSel searches for the closest structures in the Euclidean space. The method does not take into account the possible error of the secondary structure estimation. This is useful for structures lying in a rarely populated part of the secondary structure space (fold space). (ii) The algorithm searches for all the domains that lie within  $1.5 \times \text{RMSD}$  distance in each structural element from the estimated secondary structure. In other words, we look up the structures in a box centered to the BeStSel result. The size of the box is determined by the RMSD of BeStSel on SP175 reference set. The hits in the box are sorted out for classes, architectures and topologies. The resulting table shows the frequencies and percentages of the different groups in the CATH categories in the order of frequency. In the most dense regions of the secondary structural space hundreds of points can be found in the box (i.e. within the expected error of BeStSel), and the closest structures are not necessarily the correct ones. In most cases, this method provides the highest reliability. (iii) The weighted K-nearest neighbors (WKNN) (17) method: in each layer (class, architecture, topology and homology) the predicted categories are ordered by WKNN score, which is defined by the sum of the weighted distance (reverse square city block distance) of every structures (from the query point) among the K-nearest neighbors which belong to the same category.

### The operation of the BeStSel web server

The BeStSel web server is freely available for academic users. A detailed description of the use of the server is provided in the tutorial.pdf file, which is attached as Supplementary Material. The homepage also provides short helps, explanations and important tips for users. Error messages explain when data format is inappropriate. The homepage provides four program blocks: Single spectrum analysis, Fold recog-

niton, Multiple spectra analysis and Secondary structure and  $\beta$ -sheet decomposition for PDB structures. The block diagram showing the modules and functions of the web server is presented in Figure 2.

In single spectrum analysis, a single CD spectrum can be analyzed for the secondary structure composition and the protein fold can be predicted in a second step. The input is a CD spectrum either in normalized form ( $\Delta\epsilon$  or mean residue ellipticity,  $[\theta]$ ) or as measured data. In the latter case, protein concentration, number of residues and path-length data should be given, as well. The spectral data can be copied into the BeStSel text box or uploaded from a text file. Text file outputs of various instruments are usable. The program recognizes automatically the file header and the data columns. Column separator can be space, comma, semicolon or tab. The order of wavelength data is handled properly. The data step can be different from 1 nm/data, the program will convert it automatically to data in 1 nm steps. For data upload, a captcha should be provided to prevent automatic attacks from the internet. After uploading, the Data Examination page appears, where the user can verify the correct handling of the data. The secondary structure calculation is initiated with a single click. The output is a graphical presentation of the secondary structure contents and the spectral fitting with RMSD and normalized RMSD (NRMSD) data. It can be saved either in the graphical form or in text format for further data processing or figure preparation. The users can adjust the wavelength range and use a scaling factor to recalculate the results. The form of the output data can be modified for the convenience of the user.

The 'Best factor' function carries out a series of analysis by changing the current scaling factor automatically in the range of 0.5–2. This function is useful to study how the results depend on the amplitude of the CD spectrum (if there is an uncertainty in the concentration or pathlength). The factor with the lowest NRMSD should not be taken as correction for your normalized spectrum when used in the 190–250 or 200–250 nm range. The correct concentration determination is essential for accurate analysis. When 175–250 or 180–250 range is used and the best factor is significantly different from 1.0, it indicates possible normalization problems, and the factor can be taken as a suggestion.

Protein fold prediction can be initiated from the results of the CD spectrum analysis by one click. Four different types of analyses are provided. (i) Search on the entire PDB for structures with similar secondary structure composition. The closest 20 structures are shown with links to the PDB. (ii) Search on the single-domain PDB subset for the closest structures. The 10 closest domains are listed with their CATH classifications and PDB links. (iii) Search on the single-domain reference set for structures that lie within the expected error of CD spectrum analysis. A list is given for the CATH classes in the order of frequency and the 10 most frequent architectures and topologies are shown. Representative graphical images for the most frequent CATH topologies are presented. (iv) The weighted K-nearest neighbors' (WKNN) method predicts the class, architecture, topology and homology of the protein. The description of the prediction methods is presented above and in the 'Materials and Methods' section.

The second module, the 'Fold recognition' module of the server is used to predict the fold of a protein from secondary structure contents provided by the user. The calculation can be initiated after the manual input of the eight secondary structure components with the condition they sum up to 100.0% and the chain length is provided. The protein fold will be predicted by the four methods described in the first module. The output is a list of the highest ranked 1, 5, 10, and 15 CATH classes, architectures, topologies and homologies, respectively. Although the WKNN method provides the most reliable fold predictions on accurate secondary structure contents, its performance declines when there is an estimation error in the secondary structure composition. However, it is excellent for structural studies to find out the fold of model structures or structures originated from the PDB.

The third block is to analyze a series of CD spectra simultaneously, which can be useful when recording CD spectra as the function of temperature, ligand concentration, etc. Data can be copied into the text box (e.g. from a spreadsheet) or opened from a text file. Similarly to the single spectrum analysis, data can be normalized or measured. After data examination, the analysis is carried out by a single clicking. Graphical or text output both are available. Wavelength range and a scaling factor can be set for recalculation.

The fourth, 'Secondary structure and  $\beta$ -sheet decomposition for PDB structure' module calculates the secondary structure composition of known protein structures deposited in the PDB on the basis of the eight structural elements of BeStSel. For comparison, DSSP data (13) and Selcon3 (5) composition are also calculated. As input, a PDB ID should be given in four letters code format.

## RESULTS AND DISCUSSION

### Performance

The major challenge in protein CD spectroscopy is to find out, which secondary structure elements contribute to the CD signal and withdraw all the structural information buried in the spectrum. The BeStSel algorithm introduced entirely new secondary structure components by taking into account the twist of the antiparallel  $\beta$ -sheets. Altogether, it distinguishes eight secondary structure components and outperforms the previously available methods regarding any of the components (11). A great advantage of the method over the previous ones is that it can be used to estimate reliably the structure of  $\beta$ -sheet-rich proteins, including membrane proteins, protein aggregates and amyloid fibrils. On an independent set of 'problematic' proteins, calculated to a common basis of helix, antiparallel- $\beta$ , parallel- $\beta$ , overall  $\beta$ -sheet and 'turn+others' structures, the RMSDs for secondary structure estimation were proved to be 0.038, 0.050, 0.032, 0.039 and 0.033 for BeStSel, while the other methods provided RMSDs in the ranges 0.083–0.26, 0.12–0.214, 0.076–0.198, 0.068–0.23 and 0.074–0.232, respectively (11). None of the previous methods performed evenly for the different secondary structure components. BeStSel provides the highest accuracy in the SRCD range of

175–250 nm. However, its performance is still fully acceptable even in the 200–250 nm wavelength range which is often used in measurements carried out using conventional spectropolarimeters (see Micsonai *et al.* (11) for detailed statistics). However, using the narrower wavelength range needs especially accurate concentration and pathlength determination.

The orientation and twisting of  $\beta$ -sheets together with the helical and 'others' secondary structure components characterize the protein folding pattern and make the prediction of protein fold possible down to the topology/homology levels regarding the CATH protein fold classification (12). Supplementary Table S1 shows the theoretical reliability of the fold prediction calculated on the domains of CATH 4.2 (16) as secondary structure inputs in a 5-fold cross-validated manner. Supplementary Table S2 presents the performance of the various fold prediction methods on the SP175 SRCD reference set comparing the CATH 4.2 single domain set to that of CATH 3.5. The 'Box' and WKNN methods provided the highest reliability.

### Applications

CD spectroscopy of proteins, combined with the reliable secondary structure determination of BeStSel can be used to study the correct folding of recombinant proteins, experimental validation of protein models, the effect of the environmental conditions and mutations, the structure of amyloid fibrils and toxic oligomers and binding interactions. The BeStSel method was used to verify the correct fold of recombinant proteins (18,19). Tayeb-Fligelman *et al.* investigated the structural changes upon the 'cross-alpha' amyloid-like polymer formation of PSM $\alpha$ 3 peptide (20). Misra *et al.* followed the time-dependent changes in secondary structure contents upon aggregation of polyQ-A $\beta$  variants (21). Chan *et al.* analyzed the secondary structure of the amyloidogenic LARA domain of bacterial regulatory adenosine triphosphatase variant A (RavA) (22). Yamaguchi *et al.* showed that during the continuous ultrasonication the full-length mouse prion protein (PrP) forms distorted fibrils,  $\beta$ -oligomers and amorphous aggregates at different pH (23). Lin *et al.*, investigated the aggregation of cytochrome C (24). Malmos *et al.* demonstrated how glycosaminoglycans promote fibrillation of salmon calcitonin (25). Jayaraman *et al.* investigated the effect of lipid environment on amyloid fibril formation of human serum amyloid A (26). Yang *et al.* analyzed the structural changes of wild-type and mutant presenilins (PS1 and PS2) in lipid environment (27). Sahoo *et al.* studied the interaction between bovine myeloid matured cathelicidin-5 (BMAP-28) and large unilamellar vesicles (28). Terakawa *et al.* showed increased helical contents of  $\alpha$ -synuclein with the increase in the concentration of lipids of small unilamellar vesicles (29). The reliability of structural models were confirmed by CD spectroscopy and BeStSel on functional amyloid transporter from *Pseudomonas*, FapF, and its coiled coil peptide derivative (30), myoglobin and FK506 binding protein (FKBP) (31) and StI protein (32). Sajó *et al.* studied the non-cooperative thermal denaturation of FliS, the four-helix bundle flagellar chaperone protein. They found that

upon heating, first the length of the helices decreases and the number of helices starts to decrease at only at higher temperatures (33). BeStSel was used to analyze SRCD spectra of wide wavelength ranges of various proteins (32–39).

### Case studies

We present CD experiments and their analyses as relevant case studies for the use of the BeStSel web server. Thermal denaturation of human insulin was followed by recording its CD spectra at 5°C steps. BeStSel analysis showed that the main conformational change upon denaturation is the disruption of the  $\alpha$ -helices and increase of disordered conformation. The length and number of  $\alpha$ -helices are gradually decreasing in a broad temperature range to an almost total loss at 100°C (Supplementary Figure S1A–C). Kinetics of partial unfolding of human  $\beta_2$ -microglobulin Asp38Ala variant was followed by CD spectroscopy in the presence of 0.5 mM SDS. According to BeStSel, the main conformational change is a significant decrease in overall antiparallel  $\beta$ -sheet content while there was no parallel  $\beta$ -sheet detectable (Supplementary Figure S1D–F). Aggregation of amyloid- $\beta$  (1–42) peptide was followed by CD spectroscopy at 37°C. After a lagtime, we can see the formation of parallel  $\beta$ -sheet structure in parallel with the formation of the amyloid fibrils as verified by electron microscopy (Supplementary Figure S1G–I).

### NEW FEATURES

The first version of BeStSel was released in 2015 as described by Micsonai *et al.* (11) and was optimized for Firefox. The current version works on any web browser. The background databases were updated; originally it recognized 87356 PDB structures for secondary structure analysis and fold classification which is up-to-date now with 130254 structures. The updated single domain dataset used as a basis for fold prediction contains now 55350 single domains versus 10433 and based on CATH 4.2 instead of CATH 3.5. It covers 41 architectures, 1310 topologies and 5398 homologies (previously were 38, 783 and 1490, respectively). There is a fourth module for data input, users can provide arbitrary secondary structure contents and the searches for similar structures and fold prediction is carried out on these data. A fourth fold prediction method is introduced applying a WKNN search engine. While information and help are provided throughout the use of the web server, a downloadable detailed tutorial is also added.

### LIMITATIONS AND FURTHER DEVELOPMENTS

Although BeStSel provides accurate secondary structure estimation for a broad range of proteins, its eight secondary structure components do not account for some special secondary structure types. Polyproline-II helix which is characteristic of collagen-like structures, different type of turns that are often the main structural components of short peptides,  $3_{10}$ -helices which appear in higher amounts in some globular proteins are not distinguished by BeStSel and thus analysis for such structures is not adequate. BeStSel does not treat the aromatic contributions which gives some uncertainty in the case of high number of aromatic residues.

The spectra of highly disordered proteins somewhat remind the highly right-twisted antiparallel  $\beta$ -sheets (Anti3 component). When a protein have high disordered content, a part of it might be counted up as Anti3 component.

The basis spectra sets of BeStSel were optimized on a reference set of 73 proteins having high quality CD spectra and known X-ray structures (11). We are planning to increase this reference set with additional  $\beta$ -structured proteins and also with CD spectra of intrinsically disordered proteins (IDPs). For IDPs, molecular dynamics simulations give the corresponding structural ensembles. Re-optimizing BeStSel on the extended reference set will further improve its performance on  $\beta$ -structured proteins and on proteins containing larger disordered segments and on IDPs.

### CONCLUSION

The BeStSel web server applies the BeStSel method for secondary structure determination and fold prediction from the CD spectra. It takes into account the orientation and twist of the  $\beta$ -sheets which are responsible for the spectral diversity of  $\beta$ -structures. Using eight secondary structure elements, it provides a secondary structure estimation superior to previous algorithms. Moreover, the detailed secondary structure information makes it possible to predict the protein fold down to the level of topology/homology following the CATH protein fold classification. The advantages of BeStSel over the existing methods are the higher accuracy and usability for a broader range of proteins, such as  $\beta$ -structure-rich proteins, membrane proteins, aggregates, amyloid fibrils. The web server provides a user-friendly and intelligent interface for the analysis of single or multiple CD spectra to gain detailed structural information. It also provides the secondary structure composition of atomic resolution structures deposited in the PDB for reference purposes. The server is flexible with adjustable wavelength ranges, scaling of the spectra, and provides links to the corresponding PDB structures upon fold prediction. Short help messages and a tutorial facilitates its use. The server is valuable for fast and inexpensive experimental protein structure characterization in any field of protein science, structural biochemistry, biotechnology and pharmaceutical industry.

### DATA AVAILABILITY

The BeStSel web server is freely accessible at <http://bestsel.elte.hu>.

### SUPPLEMENTARY DATA

Supplementary Data are available at NAR Online.

### FUNDING

National Research, Development and Innovation Fund of Hungary [K\_120391, KH\_125597, 2017-1.2.1-NKP-2017-00002, FIEK\_16-1-2016-0005, TÉT\_16-1-2016-0134, TÉT\_16-1-2016-0197]; SOLEIL Synchrotron, France [proposals 20171582, 20160916, 20151300, 20150515]; Campus France [Balaton-Programme Hubert Curien, 38642YK];



Institute for Protein Research, Osaka University [ICR-17-02]; JSPS KAKENHI [15K18518, 25870407, 15K07038 to Y-H.L.]; Hungarian Academy of Sciences, János Bolyai Scholarship (to A.M.). Funding for open access charge: Research Grants [K\_120391, KH\_125597].

*Conflict of interest statement.* None declared.

## REFERENCES

- Greenfield, N. and Fasman, G.D. (1969) Computed circular dichroism spectra for the evaluation of protein conformation. *Biochemistry*, **8**, 4108–4116.
- Wallace, B.A. and Janes, R.W. (2001) Synchrotron radiation circular dichroism spectroscopy of proteins: secondary structure, fold recognition and structural genomics. *Curr. Opin. Chem. Biol.*, **5**, 567–571.
- Bohm, G., Muhr, R. and Jaenicke, R. (1992) Quantitative analysis of protein far UV circular dichroism spectra by neural networks. *Protein Eng.*, **5**, 191–195.
- Perez-Iratxeta, C. and Andrade-Navarro, M.A. (2008) K2D2: estimation of protein secondary structure from circular dichroism spectra. *BMC Struct. Biol.*, **8**, 25.
- Provencher, S.W. and Glockner, J. (1981) Estimation of globular protein secondary structure from circular dichroism. *Biochemistry*, **20**, 33–37.
- Sreerama, N., Venyaminov, S.Y. and Woody, R.W. (1999) Estimation of the number of alpha-helical and beta-strand segments in proteins using circular dichroism spectroscopy. *Protein Sci.*, **8**, 370–380.
- Sreerama, N. and Woody, R.W. (2000) Estimation of protein secondary structure from circular dichroism spectra: comparison of CONTIN, SELCON, and CDSSTR methods with an expanded reference set. *Anal. Biochem.*, **287**, 252–260.
- Whitmore, L. and Wallace, B.A. (2004) DICHROWEB, an online server for protein secondary structure analyses from circular dichroism spectroscopic data. *Nucleic Acids Res.*, **32**, W668–W673.
- Wiedemann, C., Bellstedt, P. and Grolach, M. (2013) CAPITO—a web server-based analysis and plotting tool for circular dichroism data. *Bioinformatics*, **29**, 1750–1757.
- Khrapunov, S. (2009) Circular dichroism spectroscopy has intrinsic limitations for protein secondary structure analysis. *Anal. Biochem.*, **389**, 174–176.
- Micsonai, A., Wien, F., Kernya, L., Lee, Y.H., Goto, Y., Refregiers, M. and Kardos, J. (2015) Accurate secondary structure prediction and fold recognition for circular dichroism spectroscopy. *Proc. Natl. Acad. Sci. U.S.A.*, **112**, E3095–E3103.
- Orengo, C.A., Michie, A.D., Jones, S., Jones, D.T., Swindells, M.B. and Thornton, J.M. (1997) CATH—a hierarchic classification of protein domain structures. *Structure*, **5**, 1093–1108.
- Kabsch, W. and Sander, C. (1983) Dictionary of protein secondary structure: pattern recognition of hydrogen-bonded and geometrical features. *Biopolymers*, **22**, 2577–2637.
- Ho, B.K. and Curmi, P.M. (2002) Twist and shear in beta-sheets and beta-ribbons. *J. Mol. Biol.*, **317**, 291–308.
- Lees, J.G., Miles, A.J., Wien, F. and Wallace, B.A. (2006) A reference database for circular dichroism spectroscopy covering fold and secondary structure space. *Bioinformatics*, **22**, 1955–1962.
- Sillitoe, I., Lewis, T.E., Cuff, A., Das, S., Ashford, P., Dawson, N.L., Furnham, N., Laskowski, R.A., Lee, D., Lees, J.G. *et al.* (2015) CATH: comprehensive structural and functional annotations for genome sequences. *Nucleic Acids Res.*, **43**, D376–D381.
- Dudani, S.A. (1976) The distance-weighted k-nearest-neighbor rule. *IEEE Trans. Syst. Man Cybern.*, **SMC-6**, 325–327.
- Saito, F., Hirayasu, K., Satoh, T., Wang, C.W., Lusingu, J., Arimori, T., Shida, K., Palacpac, N.M.Q., Itagaki, S., Iwanaga, S. *et al.* (2017) Immune evasion of *Plasmodium falciparum* by RIFIN via inhibitory receptors. *Nature*, **552**, 101–105.
- Sen Mojumdar, S., N Scholl, Z., Dee, D.R., Rouleau, L., Anand, U., Garen, C. and Woodside, M.T. (2017) Partially native intermediates mediate misfolding of SOD1 in single-molecule folding trajectories. *Nat. Commun.*, **8**, 1881.
- Tayeb-Fligelman, E., Tabachnikov, O., Moshe, A., Goldshmidt-Tran, O., Sawaya, M.R., Coquelle, N., Colletier, J.P. and Landau, M. (2017) The cytotoxic *Staphylococcus aureus* PSMalpha3 reveals a cross-alpha amyloid-like fibril. *Science*, **355**, 831–833.
- Misra, P., Kodali, R., Chemuru, S., Kar, K. and Wetzel, R. (2016) Rapid alpha-oligomer formation mediated by the Abeta C terminus initiates an amyloid assembly pathway. *Nat. Commun.*, **7**, 12419.
- Chan, S.W., Yau, J., Ing, C., Liu, K., Farber, P., Won, A., Bhandari, V., Kara-Yacoubian, N., Seraphim, T.V., Chakrabarti, N. *et al.* (2016) Mechanism of Amyloidogenesis of a Bacterial AAA+ Chaperone. *Structure*, **24**, 1095–1109.
- Yamaguchi, K.I., Honda, R.P., Elhelaly, A.E. and Kuwata, K. (2018) Acceleration of nucleation of prion protein during continuous ultrasonication. *J. Biochem.*, **163**, 503–513.
- Lin, Y., Kardos, J., Imai, M., Ikenoue, T., Kinoshita, M., Sugiki, T., Ishimori, K., Goto, Y. and Lee, Y.H. (2016) Amorphous aggregation of cytochrome c with inherently low Amyloidogenicity is characterized by the Metastability of Supersaturation and the phase diagram. *Langmuir*, **32**, 2010–2022.
- Malmos, K.G., Bjerring, M., Jessen, C.M., Nielsen, E.H., Poulsen, E.T., Christiansen, G., Vosegaard, T., Skrydstrup, T., Enghild, J.J., Pedersen, J.S. *et al.* (2016) How Glycosaminoglycans promote fibrillation of salmon calcitonin. *J. Biol. Chem.*, **291**, 16849–16862.
- Jayaraman, S., Gantz, D.L., Haupt, C. and Gursky, O. (2017) Serum amyloid A forms stable oligomers that disrupt vesicles at lysosomal pH and contribute to the pathogenesis of reactive amyloidosis. *Proc. Natl. Acad. Sci. U.S.A.*, **114**, E6507–E6515.
- Yang, G., Yu, K., Kaitatzi, C.S., Singh, A. and Labahn, J. (2017) Influence of solubilization and AD-mutations on stability and structure of human presenilins. *Sci. Rep.*, **7**, 17970.
- Sahoo, B.R., Maruyama, K., Edula, J.R., Tougan, T., Lin, Y., Lee, Y.H., Horii, T. and Fujiwara, T. (2017) Mechanistic and structural basis of bioengineered bovine Cathelicidin-5 with optimized therapeutic activity. *Sci. Rep.*, **7**, 44781.
- Terakawa, M.S., Lee, Y.H., Kinoshita, M., Lin, Y., Sugiki, T., Fukui, N., Ikenoue, T., Kawata, Y. and Goto, Y. (2018) Membrane-induced initial structure of alpha-synuclein control its amyloidogenesis on model membranes. *Biochim. Biophys. Acta*, **1860**, 757–766.
- Rouse, S.L., Hawthorne, W.J., Berry, J.L., Cherev, D.S., Ionescu, S.A., Lambert, S., Stylianou, F., Ewert, W., Mackie, U., Morgan, R.M.L. *et al.* (2017) A new class of hybrid secretion system is employed in *Pseudomonas* amyloid biogenesis. *Nat. Commun.*, **8**, 263.
- Brodie, N.I., Popov, K.I., Petrotchenko, E.V., Dokholyan, N.V. and Borchers, C.H. (2017) Solving protein structures using short-distance cross-linking constraints as a guide for discrete molecular dynamics simulations. *Sci. Adv.*, **3**, e1700479.
- Nyiri, K., Kohegyi, B., Micsonai, A., Kardos, J. and Vertessy, B.G. (2015) Evidence-Based structural model of the staphylococcal repressor protein: separation of functions into different domains. *PLoS One*, **10**, e0139086.
- Sajo, R., Toke, O., Hajdu, I., Jankovics, H., Micsonai, A., Dobo, J., Kardos, J. and Vonderviszt, F. (2016) Structural plasticity of the *Salmonella* Flis flagellar export chaperone. *FEBS Lett.*, **590**, 1103–1113.
- Bizouarn, T., Karimi, G., Masoud, R., Souabni, H., Machillot, P., Serfaty, X., Wien, F., Refregiers, M., Houee-Levin, C. and Baciou, L. (2016) Exploring the arachidonic acid-induced structural changes in phagocyte NADPH oxidase p47(phox) and p67(phox) via thiol accessibility and SRCD spectroscopy. *FEBS J.*, **283**, 2896–2910.
- Hussain, R., Hughes, C.S., Javorfi, T., Siligardi, G., Williams, P. and Bonev, B.B. (2018) To Boil an Egg: Substrate binding affects critical stability in thermal unfolding of proteins. *J. Phys. Chem. B*, **122**, 2213–2218.
- Nasser, S., Hedoux, A., Giuliani, A., Le Floch-Fouere, C., Sante-Lhoutellier, V., de Waele, I. and Delaplace, G. (2017) Investigation of secondary structure evolution of micellar casein powder upon aging by FTIR and SRCD: consequences on solubility. *J. Sci. Food Agric.*, **98**, 2243–2250.
- Nemeth, E., Balogh, R.K., Borsos, K., Czene, A., Thulstrup, P.W. and Gyurcsik, B. (2016) Intrinsic protein disorder could be overlooked in cocrystallization conditions: an SRCD case study. *Protein Sci.*, **25**, 1977–1988.
- Souabni, H., Wien, F., Bizouarn, T., Houee-Levin, C., Refregiers, M. and Baciou, L. (2017) The physicochemical properties of membranes correlate with the NADPH oxidase activity. *Biochim. Biophys. Acta*, **1861**, 3520–3530.



39. Townsend,D., Hughes,E., Hussain,R., Siligardi,G., Baldock,S., Madine,J. and Middleton,D.A. (2017) Heparin and methionine oxidation promote the formation of Apolipoprotein A-I amyloid comprising alpha-Helical and beta-Sheet Structures. *Biochemistry*, **56**, 1632–1644.
40. Whitmore,L., Woollett,B., Miles,A.J., Janes,R.W. and Wallace,B.A. (2010) The protein circular dichroism data bank, a Web-based site for access to circular dichroism spectroscopic data. *Structure*, **18**, 1267–1269.
41. Luhrs,T., Ritter,C., Adrian,M., Riek-Loher,D., Bohrmann,B., Dobeli,H., Schubert,D. and Riek,R. (2005) 3D structure of Alzheimer's amyloid-beta(1-42) fibrils. *Proc. Natl. Acad. Sci. U.S.A.*, **102**, 17342–17347.
42. Iwata,K., Matsuura,T., Sakurai,K., Nakagawa,A. and Goto,Y. (2007) High-resolution crystal structure of beta2-microglobulin formed at pH 7.0. *J. Biochem.*, **142**, 413–419.
43. De Meester,P., Brick,P., Lloyd,L.F., Blow,D.M. and Onesti,S. (1998) Structure of the Kunitz-type soybean trypsin inhibitor (STI): implication for the interactions between members of the STI family and tissue-plasminogen activator. *Acta Crystallogr. D Biol. Crystallogr.*, **54**, 589–597.